Evidence for Determinism in Ventricular Fibrillation

7 authors, including:

Mark L. Spano
Arizona State University
130 PUBLICATIONS   6,581 CITATIONS

William Ditto
North Carolina State University
218 PUBLICATIONS   10,376 CITATIONS

Daniel Kaplan
Macalester College
93 PUBLICATIONS   5,556 CITATIONS

Evidence for Determinism in Ventricular Fibrillation

Francis X. Witkowski,[1] Katherine M. Kavanagh,[1] Patricia A. Penkoske,[1] Robert Plonsey,[2] Mark L. Spano,[3]
William L. Ditto,[4] and Daniel T. Kaplan[5]

[1]University of Alberta, Edmonton, Alberta, Canada T6G 2R7
[2]Department of Biomedical Engineering, Duke University, Durham, North Carolina, 27708-0281
[3]Naval Surface Warfare Center, Silver Spring, Maryland 20903
[4]School of Physics, Georgia Institute of Technology, Atlanta, Georgia, 30332-0430
[5]Department of Physiology, McGill University, Montreal, Quebec, Canada H3G 2Y6
(Received 9 September 1994; revised manuscript received 16 November 1994)

Using a recently formulated technique for *in vivo* cardiac transmembrane current estimation, we examined ventricular fibrillation for evidence of deterministic linear and nonlinear structure. Both unstable fixed point analysis and a newly formulated measure of nonlinear determinism indicated that ventricular fibrillation *in vivo* exhibits deterministic dynamics similar to those previously used in chaos control.

PACS numbers: 87.22.–q, 05.45.+b, 87.45.Bp

Ventricular fibrillation (VF) is a frenzied and irregular heart rhythm disturbance that renders the heart incapable of sustaining life [1]. VF is always fatal within minutes unless externally terminated by the passage of a large electrical current through the heart muscle. The use of "chaos control" techniques to stabilize small patches of heart tissue has been reported [2], and recent theoretical work suggests that similar strategies may be applicable to spatially extended systems such as ventricular fibrillation (VF) in the whole heart [3].

In prior analysis of experimental data VF has often been treated as a random and irregular process. This approach precludes the development of feedback control strategies that would use small stimuli to terminate VF. For this reason, it is important to uncover any deterministic dynamics that underlie VF. Here we report that by using a new technique for measuring cardiac transmembrane current (I_m)

in vivo [4,5], and by applying recently developed methods for the identification of deterministic structure in time series [6], we have found evidence for deterministic dynamics in VF. The same sort of dynamics has been successfully exploited in the control of physical and biological chaotic systems [2,7–14]. The presence of observably deterministic dynamics from excitable cardiac tissue has been controversial [15–20].

Our experimental preparations consisted of open-chest anesthetized dogs, whose hearts were studied *in vivo* after VF was electrically induced [5]. I_m was measured from ventricular epicardium without cell disruption. Using this experimental technique, we have recently been able to reliably differentiate propagated electrical activation from passive electrotonic alterations [5]. This effectively identifies local electrophysiological events for subsequent analysis. The ratio of the areas derived from
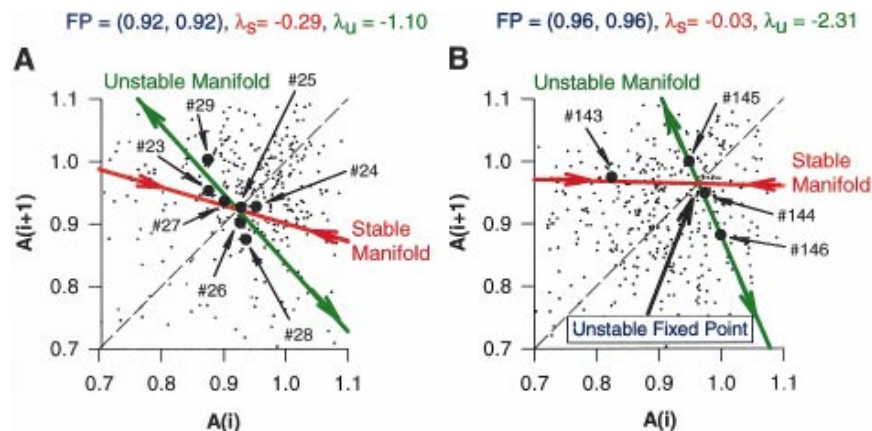

FIG. 1. (a) Return plot of the time series generated by the ratio of negative to positive area $A(i)$ under the transmembrane current for a typical 1 min interval of *in vivo* ventricular fibrillation illustrating the local structure of the chaotic attractor. The range of data displayed was narrowed to more clearly demonstrate the points contributing to the local structure. Note the flip saddle structural appearance for points 23 through 29. Coordinates for the calculated unstable fixed point (FP), stable eigenvalue (λ_s), and unstable eigenvalue (λ_u) for this visitation of the unstable fixed point are provided above the plot. Diagonal dashed line is the line of identity [$A(i + 1) = A(i)$]. (b) Another saddle structure [points 143–146] generated by a second representative VF time series with abbreviations as in (a).

the inwardly and outwardly directed I_m, $A(i)$, as well as the deflection-to-deflection interval $D(i)$, was computed for each nonelectrotonic deflection [i.e., $A(i) > 0$] during VF, where $i = 1, 2, \ldots,$ indexes the deflection number. The 30 episodes of VF analyzed provided 17 125 deflections for analysis.

Initial examination for evidence of determinism in these time series involved return plots of $A(i + 1)$ versus $A(i)$ and of similarly plotted interval data during the course of VF (see Fig. 1). The shape of the cloud of points in such a two-dimensional plot does not reveal any simple dependence of $A(i + 1)$ on $A(i)$. However, the sequence of points does suggest the existence of a deterministic mechanism involving an unstable fixed point [2,7–10]. A fixed point may occur only when $A(i + 1) = A(i)$.

A type of unstable fixed point often encountered in chaotic systems is a "saddle." There is a fixed point at the center of the saddle, and stable and unstable manifolds that intersect at the fixed point. In a two-dimensional plot of this kind, the slopes of the stable and unstable manifolds at the fixed point are numerically equal to the eigenvalues of their respective manifolds at the fixed point. If the state of the system, as represented by a point in the $[A(i), A(i + 1)]$ plane, is quite close to the stable manifold but not close to the fixed point, subsequent iterates will first move closer toward the fixed point along the stable manifold and then move away along the unstable manifold as indicated in the sequences shown in Fig. 1. In analyzing experimental data, where the directions or even the existence of the manifolds are not known *a priori,* we invert the above logic and use the presence of such a sequence of points as the initial evidence for the existence of a fixed point and related stable and unstable manifolds.
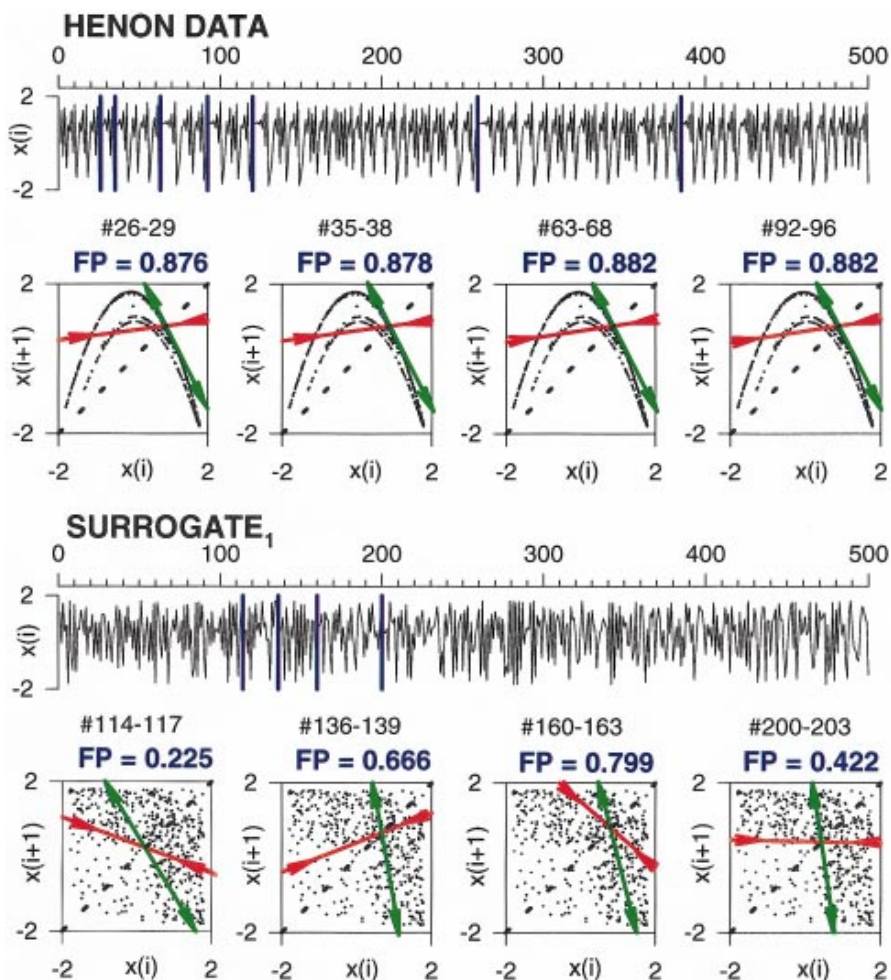

FIG. 2. Time series for the Henon map, $\{x(i + 1) = 1.4 + 0.3y(i) - x(i)^2, y(i + 1) = x(i)\}$, with seven visitations to the fixed point automatically detected by scanning the time series (vertical lines). Return plots for the first four visitations presented below with their respective stable and unstable manifolds. For the Henon map, the unstable fixed point is known to be characterized by fixed point = 0.884, $\lambda_u = -1.924$. From scanning the time series FP = 0.882 ± 0.0002 and $\lambda_u = -1.973 ± 0.007$. The second time series, labeled Surrogate$_1$, is an example of one of the 10 surrogates formed from the Henon time series. When this surrogate time series is scanned, four putative fixed points are obtained, which demonstrate a marked variation in both fixed point location and architecture. Statistical significance between this Henon time series and the mean of 10 surrogates was found to have a sigma value >50. When varying amounts of white noise were added to the Henon data, the ability to discern a difference between it and its surrogates deteriorated; at 20% added noise the sigmal value = 3.6, and at 25% added noise it was less than 3.

A typical example of such a sequence from an episode of VF is demonstrated by following state points 23–29 in Fig. 1(a). From points 23 to 25, the state of the system is drawn toward the unstable fixed point along the stable manifold. Points 26 through 29 demonstrate exponential divergence away from the fixed point along the unstable manifold. A single visitation of an unstable fixed point from another run of VF is shown in Fig. 1(b) for which we calculated (from 3 visitations) a fixed point $= 0.971 \pm 0.007$, $\lambda_u = -1.70 \pm 0.53$, and $\lambda_s = -0.14 \pm 0.10$ (mean $\pm$ standard deviation). Evidence for at least three full sequences with the structure of Fig. 1 in each 1 min duration time series was observed in 24/30 VF episodes when examining $A(i)$ and 19/30 episodes when examining $D(i)$, with a maximum of six sequences observed in any time series.

Sequences of points moving inward along a line and outward along another line can be observed in random data. Figure 2 shows data from the Henon map, which is known to have a fixed point at 0.884, consistent with the sequences observed in the data. Examining surrogate data generated from the Henon map also reveals sequences that resemble fixed points. The surrogate data is constructed by shuffling the original time series in a random manner that preserves the autocorrelation function of the original data, and is equivalent to forcing a linear autoregressive model with white noise [21]. The fixed points identified in the surrogate data shown in Fig. 2 are dynamically spurious, and arise from occasional chance correlations between successive data points. Note that the location of the putative fixed point and the slope of the unstable manifold vary greatly from sequence to sequence in the surrogate data, but are largely the same in the Henon data.

In order to establish whether the fixed-point sequences observed in the fibrillation data arise from chance, we adopted the following procedure for each time series:

(1) The data was scanned for all sequences resembling fixed point dynamics.

(2) For each such sequence, the location of the putative fixed point and the unstable eigenvalue were calculated by least mean squares fit.

(3) From all the fixed-point sequences in each time series, the three were selected that minimized the product of the variance of the location of the fixed point and the variance of the unstable eigenvalues. The inverse of this minimized product of variances was then used as a discriminating statistic in a surrogate data test.

(4) Ten different realizations of surrogate data were constructed from the fibrillation time series, and steps (1)–(3) were carried out on each of the surrogate data realizations.
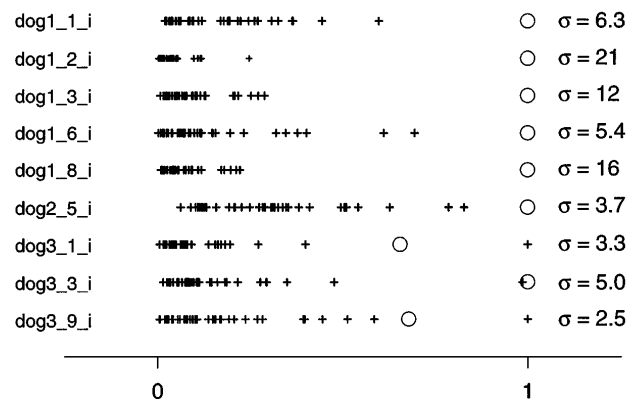
(5) The 10 values of the discriminating statistic for the surrogate data were compared to the value of the discriminating statistic for the original time series and was deemed significant when the data was different than the mean value for the 10 surrogates by more than 3 standard deviations ($\sigma > 3$).

This procedure yielded positive results in 5/30 VF episodes when examining $A(i)$ and 9/30 episodes when examining $D(i)$. As an additional nonparametric examination for significance, the discriminating statistic for the nine episodes of $D(i)$ initially deemed significant were simply plotted against the identically derived statistic for 39 surrogates. If the value for the original time series was greater than the values for all 39 surrogates, we judge that a statistically significant difference between the original and the surrogates has been found at the roughly 2.5% significance level. This final procedure yielded the results shown in Fig. 3, where 9/9 of the $D(i)$ time series fulfilled this nonparametric criterion at the 0.05 significance level.

To further globally test for the existence of deterministic nonlinear dynamics, we employed a quantitative method that has proven effective on short data sets from random appearing but deterministic systems [6]. The analysis is based on the idea that in a deterministic system, the dynamical rule will be such that nearby states will have similar changes in state with time. The test evaluates evidence for this in the time series by calculating the distance r between all pairs of reconstructed state space points and the distance e between the successive values [6]. For a perfectly deterministic system, the resulting curve of e vs r should slope toward $e = 0$ at $r = 0$ [6]. Again, we control for statistical fluctuations in the finite length time series by using surrogate data [21].

When this analysis was applied to the $A(i)$ and $D(i)$ time series generated by the 30 VF episodes, evidence for nonlinear determinism was found in 7/30 when examining $A(i)$ and 20/30 when $D(i)$ was examined. Evidence of nonlinear determinism was deemed statistically significant when $e(r = 0)$ for the data was lower than $e(r = 0)$ for the surrogates by more than 3 standard deviations at embedding dimension 3 as shown in Fig. 4. We also

Normalized unstable fixed point ranking

open circle = VF interval data, + = surrogate values (39 surrogates)

FIG. 3. Unstable fixed point discriminating statistic for the nine ventricular fibrillation $D(i)$ time series (with initial $\sigma > 3$ for 10 surrogates) and their corresponding 39 autocorrelation matched surrogates. Note that only 1/9 time series, when using 39 surrogates, had a σ that fell below 3.
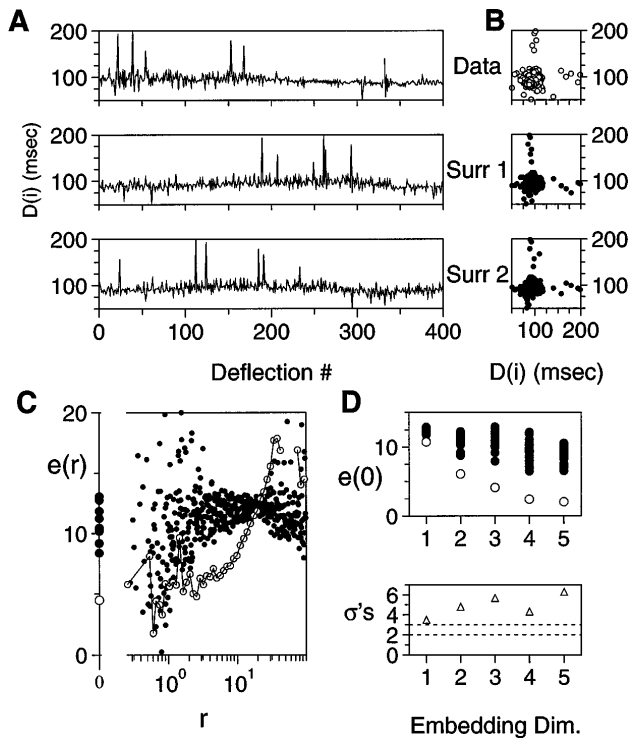
FIG. 4. (a) Interdeflection interval $D(i)$ time series (top frame), and two surrogate data time series with the same histogram and autocorrelation function. (b) The return plot $D(i + 1)$ versus $D(i)$ for the time series in (a). (c) e versus r (calculated as previously described [6]) for the $D(i)$ time series (open circles) and 10 surrogate data sets. The considerable spread of the surrogates for small r is due to the short length of the time series. The projection to $e(r = 0)$ is shown on the left-hand axis. An imbedding dimension of 3 is used here. (d) $e(r = 0)$ versus embedding dimension for the $D(i)$ time series (open circles) and the surrogates. The bottom frame shows the deviation of $e(r = 0)$ of the $D(i)$ time series from the mean of $e(r = 0)$ of the surrogates, in terms of the standard deviation of the surrogates. A deviation of >3 standard deviations at embedding dimension 3 was the criterion used for statistical significance.

analyzed the $A(i)$ and $D(i)$ time series using two other nonlinear statistics: mean log prediction error and correlation dimension [21]. Similar overall results were obtained. The increased proportion of positive results when compared to the unstable fixed point analysis most likely reflects the improved noise immunity of the technique. As an example, the evidence for nonlinear determinism was readily detected in the Henon data with additive noise levels of up to 50%, but significance by the unstable fixed point technique could only be demonstrated up to 20% added noise.

The two complementary approaches described above, one of which tests for local determinism and the other for global determinism, clearly indicate that there are strong deterministic components to VF. The deterministic components are similar to those identified in other chaotic systems in which control was possible [2,7–10]. A major point of this study is that VF is perhaps not best understood in terms of the low-dimension versus high-dimension

paradigm that has dominated nonlinear dynamics data analysis for the past decade. Instead, we present evidence that VF contains episodes of simple dynamics interwoven with a background of much more complicated dynamics. Although the work here suggests that the dynamics of VF might be amenable to chaotic control techniques, the practical implementation of such control is still highly speculative and will present significant challenges.

[1] M. S. Eisenberg, A. Hallstrom, and L. Bergner, N. Engl. J. Med. **306**, 1340 (1982).

[2] A. Garfinkel, M. L. Spano, W. L. Ditto, and J. N. Weiss, Science **257**, 1230 (1992).

[3] I. Aranson, H. Levine, and L. Tsimring, Phys. Rev. Lett. **72**, 2561 (1994).

[4] F. X. Witkowski, K. M. Kavanagh, P. A. Penkoske, and R. Plonsey, Circ. Res. **72**, 424 (1993).

[5] F. X. Witkowski, R. Plonsey, P. A. Penkoske, and K. M. Kavanagh, Circ. Res. **74**, 507 (1994).

[6] D. T. Kaplan, Physica (Amsterdam) **73D**, 38 (1994).

[7] E. Ott, C. Grebogi, and J. A. Yorke, Phys. Rev. Lett. **64**, 1196 (1990).

[8] W. L. Ditto, S. N. Rauseo, and M. L. Spano, Phys. Rev. Lett. **65**, 3211 (1990).

[9] W. L. Ditto and L. M. Pecora, Sci. Am. **269**, No. 2, 78 (1993).

[10] T. Shinbrot, C. Grebogi, E. Ott, and J. A. Yorke, Nature (London) **363**, 411 (1993).

[11] R. Roy, T. W. Murphy, Jr., T. D. Maier, Z. Gills, and E. R. Hunt, Phys. Rev. Lett. **68**, 1259 (1992).

[12] E. R. Hunt, Phys. Rev. Lett. **67**, 1953 (1991).

[13] V. Petrov, V. Gaspar, J. Masere, and K. Showalter, Nature (London) **361**, 240 (1993).

[14] S. J. Schiff, K. Jerger, D. H. Duong, T. Chang, M. L. Spano, and W. L. Ditto, Nature (London) **370**, 615 (1994).

[15] M. R. Guevara, L. Glass, and A. Schrier, Science **214**, 1350 (1981).

[16] A. L. Goldberger, V. Bhargava, B. J. West, and A. J. Mandell, Physica (Amsterdam) **19D**, 282 (1986).

[17] D. R. Chialvo, R. S. Gilmour, Jr., and J. Jalife, Nature (London) **343**, 653 (1990).

[18] D. T. Kaplan and R. J. Cohen, Circ. Res. **67**, 886 (1990).

[19] F. X. Witkowski and P. A. Penkoske, in *Mathematical Approaches to Cardiac Arrhythmias,* edited by J. Jalife (New York Academy of Sciences, New York, 1990), p. 219.

[20] P. V. Bayly *et al.,* J. Cardiovasc. Electrophys. **4**, 533 (1993).

[21] J. Theiler, S. Eubank, A. Longtin, B. Galdrikian, and J. D. Farmer, Physica (Amsterdam) **58D**, 77 (1992).